

## Steady high subsonic plane compressible flows Finite elements solution by streamline perturbation

S. F. SHEN and H. C. CHEN (NEW YORK)

TWO FINITE element programs for two-dimensional subsonic compressible flows have been developed which are shown to be rapid, accurate, and flexible up to the transonic regime, including the prediction of locally supersonic pockets. The computation domain uses the incompressible velocity potential and stream function as Cartesian coordinates. A thin-airfoil type expansion is carried out, effectively to look for the solution as a perturbation of the incompressible streamline pattern. One of the two programs is for the stream function with 6-node quadratic triangular elements, and the other for the velocity potential with 9-parameter cubic triangular elements. Test cases include the Emmons nozzle, the circular cylinder, the 10% ellipse, and several symmetrical airfoils, all carried to the transonic regime. As the sonic condition is locally approached, the velocity potential program is to be preferred because of the necessary iteration for the local Mach number, and the more accurate velocity field from the cubic element used. The same programs can be used for other problems as long as the incompressible field is known or can be constructed, with no restriction to shape or thickness.

Przygotowano dwa programy rozwiązywania dwuwymiarowych zagadnień ściśliwych przepływów poddźwiękowych metodą elementów skończonych. Jak się okazało programy te są szybkie, dokładne i mogą być z powodzeniem wykorzystane aż do obszarów naddźwiękowych, z przewidzeniem lokalnie naddźwiękowych „kieszoni” włącznie. W trakcie obliczeń jako nowe współrzędne kartezjańskie przyjęto nieściśliwy potencjał prędkości i funkcję prądu. Dokonano rozwinięcia rozwiązania tak jak dla cienkiego profilu lotniczego. Efektywnie poszukiwano rozwiązania, stosując perturbację nieściśliwego modelu linii prądu. Jeden z dwóch programów służy do rozwiązywania równania na funkcję prądu przy przyjęciu elementów kwadratowo-trójkątnych o sześciu węzłach każdy. Program drugi rozwiązuje równanie dla potencjału prędkości z sześciennotrójkątnymi elementami o dziewięciu parametrach każdy. Jako przypadki testowe rozpatrzono dyszę Emmonsa, walec kołowy, 10% elipsę i wiele symetrycznych profili lotniczych, przy czym wszystkie obliczenia prowadzono aż do zakresu naddźwiękowego. Przy zbliżaniu się lokalnie do prędkości dźwięku, lepszy, jak się okazuje, jest program na potencjał prędkości z uwagi na stosowanie niezbędnej iteracji lokalnej liczby Macha i uzyskiwanie dokładniejszego pola prędkości dzięki użyciu elementu sześciennego. Ten sam program można z powodzeniem wykorzystać do obliczenia numerycznego innych zagadnień, o ile obszar nieściśliwy jest znany lub łatwy do skonstruowania bez jakichkolwiek ograniczeń jego kształtu lub grubości.

Изготовлены две программы решения двумерных задач сжимаемых дозвуковых течений методом конечных элементов. Как оказалась эти программы быстрые, точные и могут быть с успехом использованы вплоть до сверхзвуковых областей с предвидением локально сверхзвуковых „карманов” включительно. В процессе расчетов как новые декартовы координаты приняты несжимаемый потенциал скорости и функция тока. Проведено разложение решения как для тонкого авиационного профиля. Эффективно ищется решение применяя возмущение несжимаемой модели линий тока. Одна из двух программ служит для решения уравнения для функции тока, при принятии квадратнотрехугольных элементов с 6 узлами каждый. Вторая программа решает уравнение для потенциала скорости с кубическо-треугольными элементами с 9 параметрами каждый. Как тестовые случаи рассмотрены сопло Эммонса, круговой цилиндр, 10% эллипс и много симметричных авиационных профилей, причем все расчеты проведены вплоть до сверхзвуковой области. При сближении локально к скорости звука лучшей программой, как оказывается, является программа для потенциала скорости из-за применения необходимой локальной итерации числа Маха и получения более точного поля скорости благодаря использованию кубического элемента. Эту самую программу можно с успехом использовать для численного расчета других задач, если несжимаемая область известна или легко ее можно построить без никаких ограничений на ее форму или толщину.

## 1. Introduction

RECENT interest by the aircraft industry plus the increasing capacity of the high speed computers have led to great progress in the numerical computation of transonic flows. A number of highly effective finite-difference schemes [1, 2, 3, 4] are well established, especially for the two-dimensional airfoil problem. Some of them can handle even the difficult task of locating the weak shock springing from the body surface. Another approach via Dorodnitsyn's multi-strip method of integral relations [4, 5, 6, 7, 8] also produced several interesting case studies with encouraging results. The hope is to economize the computation by a decrease of the number of the unknowns. The method of integral relations may be regarded as basically of the same nature as the semi-discrete version of the finite element method, both using interpolation for the unknown in one of the coordinates and controlling the accuracy in some average integral sense. To achieve further economy, then, it seems logical that the finite element method should be explored for similar applications.

The finite element method, in theory and in practice, performs best for linear partial differential equations of the elliptic type, for which a variational principle exists and is easy to implement numerically. Highly popular, with justification, in the treatment of structures of complex geometry in solid mechanics, it has yet to receive serious consideration from aerodynamicists. No doubt the reason is partly the advanced state of other numerical methods already tested and at our disposal. Although its potential of savings in the computing cost may be luring, the feasibility should first be proved. For compressible flows, up to the transonic regime, the governing equation is highly non-linear and may not remain elliptic everywhere. Whenever a shock wave appears, its unknown location and the discontinuity of the solution cannot be conveniently described by simple interpolation. Even restricted to shockless flows, a variational principle may exist but is of little consolation: The functional involves a highly transcendental integrand, and previous attempts in the test case of the flow over a circular cylinder, starting with WANG [9] and more recently by GREENSPAN and JAIN [10] and RASMUSSEN [11], are all heavily time-consuming. Whenever the critical Mach number is exceeded and locally supersonic flow takes place, any numerical procedure, following the variational principle, trying to get at the solution as that of a boundary value problem can further be challenged with good reason.

It is apparent, as we have stressed in a review [12] earlier, that forethought and analysis must first be given to the peculiarities of the flow in question, in order to reach a workable and efficient finite element formulation. The governing equation may be cast in different forms, the resulting non-linear algebraic systems, from the variational principle or otherwise, must be solved by iteration, and the success or ease in arriving at the answer may greatly vary. An obviously straightforward approach to the compressible flow problem, for example, is to write the governing equations for the streamfunction or the velocity potential as a Poisson equation, equivalent to an incompressible flow with a spatial distribution of sources in which all terms due to compressibility are dumped. Regarding the source terms as known in an iteration process, the variational principle and its finite element treatment for the Poisson equation is simple and straightforward. Such a scheme has been adopted by many investigators [13, 14, 15, 16]. As the numerical

counterpart of the Rayleigh-Janzen expansion, it is quite satisfactory for low Mach number flows, but most definitely and rapidly deteriorates as the Mach number goes up. The replacement of the operator by a Laplacian is evidently too crude, and in regions of supersonic flow not even qualitatively correct.

Our studies in the finite element method for high subsonic flows therefore give considerable attention to rewriting the differential equation before the formal aspects of reducing it to an algebraic system are carried out. In one method, the operator is approximated in each element as that for small perturbations about a local uniform flow, i.e., a locally defined Prandtl-Glauert approximation. The finite element procedure is carried out in the physical plane for each element and then the elements are properly assembled. This investigation and some of its applications have been reported by SHEN and HABASHI [17, 18].

We describe in the following a second method, which is built upon the choice of the incompressible velocity potential and streamfunction, for the same flow under consideration, as the coordinates in the working plane where computations are to be made. The very same coordinate system was used by EMMONS in his pioneering numerical calculation of the nozzle flow [19], to map the computation domain into a rectangular strip. An interesting feature turns out to be that all streamlines, for whatever body shape, are nearly horizontal in the working plane. It immediately suggests a perturbation scheme, in the nature of a "thin-airfoil" approximation (but in the working plane and with no restriction on the actual thickness of the body). Hence the method is referred to as "streamline perturbation". The finite element programs are then developed, and found to be highly efficient, as well as flexible for easy modification to treat many other problems. More details can be found in CHEN [16].

As regards shock-fitting, in spite of the apparent success reported by CHAN and BRASHEARS [35], we have not yet developed an effective technique to our own satisfaction.

## 2. Formulation of the problem

### 2.1. Governing equations and the boundary conditions

For two-dimensional steady irrotational flow of a compressible fluid, the governing equation may be written either in terms of the stream function  $\psi$  or the velocity potential  $\phi$ . In Cartesian coordinates  $(x, y)$ , we have

$$(2.1) \quad \left(\frac{1}{\rho} \psi_x\right)_x + \left(\frac{1}{\rho} \psi_y\right)_y = 0$$

and alternatively,

$$(2.2) \quad (\rho \phi_x)_x + (\rho \phi_y)_y = 0,$$

where  $\rho$  is the density, related to the velocity field through the relation

$$(2.3) \quad \frac{\rho}{\rho_0} = \left[1 - \frac{\gamma-1}{2} \left(\frac{q}{c_0}\right)^2\right]^{\frac{1}{\gamma-1}},$$

$\gamma$  being the ratio of specific heats,  $\rho_0$  and  $c_0$  denoting, respectively, the reference density and speed, both evaluated at the stagnation condition, and  $q$  being the local speed defined

$$(2.4) \quad \frac{q}{c_0} = \frac{\rho_0}{\rho} (\psi_x^2 + \psi_y^2)^{1/2} = (\phi_x^2 + \phi_y^2)^{1/2}.$$

It will be assumed that the incompressible case for the flow in question has been obtained by other means, in terms of a complex potential  $w(z)$ , say,

$$(2.5) \quad \begin{aligned} w(z) &= \xi(x, y) + i\eta(x, y), \\ z &= x + iy. \end{aligned}$$

Clearly  $\xi$  is the incompressible velocity potential and  $\eta$  the incompressible stream function, in the usual convention. As a consequence, the velocity field  $(u_i, v_i)$  and the local speed  $Q$  follows

$$(2.6) \quad \begin{aligned} u_i &= \xi_x = \eta_y, & v_i &= \xi_y = -\eta_x, \\ Q &= (u_i^2 + v_i^2)^{1/2} = (\xi_x^2 + \xi_y^2)^{1/2} = (\eta_x^2 + \eta_y^2)^{1/2}. \end{aligned}$$

Following Emmons' treatment of the nozzle problem [19], we introduce  $\xi, \eta$  as the new coordinates. The body contour is thus reduced to a line segment along the line  $\eta = \text{const}$ . In the "working plane" with the  $\xi, \eta$ -coordinates, the velocity components  $u, v$  along the  $x$ - and  $y$ -axis directions in the physical plane are defined by

$$(2.7) \quad \begin{aligned} \frac{u}{c_0} &= \frac{\rho_0}{\rho} (v_i \psi_\xi + u_i \psi_\eta) = u_i \phi_\xi - v_i \phi_\eta, \\ \frac{v}{c_0} &= -\frac{\rho_0}{\rho} (u_i \psi_\xi - v_i \psi_\eta) = v_i \phi_\xi + u_i \phi_\eta, \end{aligned}$$

so that the local speed  $q (= \sqrt{u^2 + v^2})$  can be evaluated as

$$(2.8) \quad \frac{q}{Q} = \frac{\rho_0}{\rho} c_0 (\psi_\xi^2 + \psi_\eta^2)^{1/2} = c_0 (\phi_\xi^2 + \phi_\eta^2)^{1/2}.$$

The governing equations, Eq. (2.1) and Eq. (2.2), become respectively

$$(2.9) \quad \left( \frac{1}{\rho} \psi_\xi \right)_\xi + \left( \frac{1}{\rho} \psi_\eta \right)_\eta = 0$$

and

$$(2.10) \quad (\rho \phi_\xi)_\xi + (\rho \phi_\eta)_\eta = 0.$$

The non-linearity of Eq. (2.9) and (2.10) arises from the density  $\rho$ , which must be obtained through Eqs. (2.3) and (2.8). As already mentioned, the incompressible solution is taken as given, therefore  $Q$  as a function of  $\xi$  and  $\eta$  is known.

For the boundary conditions, let us illustrate by means of two typical cases:

i) *The internal flow through a nozzle* (Fig. 1).

Let the shape of the nozzle be given, together with the suitable entrance and exit conditions, so that the incompressible potential flow can be prescribed on and within the contour  $ABCD$ . In the working plane, the domain  $ABCD$  becomes a rectangular strip if  $AD$  and  $BC$  are chosen to be equipotential lines in the incompressible case. The constant val-

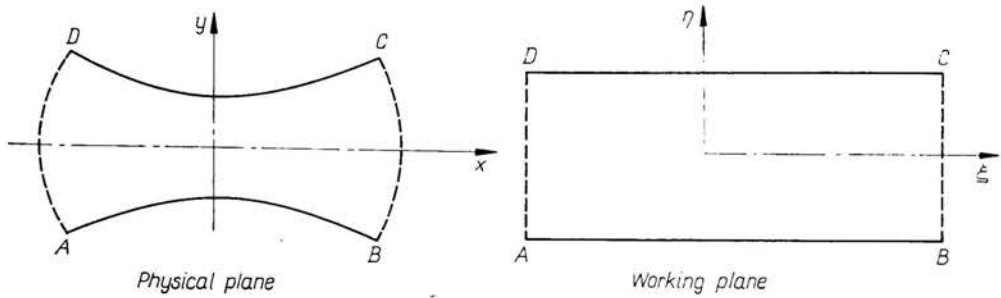


FIG. 1. Physical and working planes; nozzle.

ues of  $\eta$  along  $AB$  and  $DC$  are known, but conditions along  $AD$  and  $BC$  for the compressible case have to be specified with care: both are required if the entrance and exit flows are subsonic, but the conditions along  $BC$  must be left free when the flow exits supersonically. Furthermore, for a nozzle of finite length, the conditions cannot be arbitrarily assigned but should be reckoned together with the reservoirs, for instance, both upstream and downstream. In the example calculated by EMMONS [19], the contours  $AB$  and  $CD$  are portions of hyperbolas extending to infinity, described by

$$(2.11) \quad y^2 - x^2 \tan^2 \eta_w = \sin^2 \eta_w$$

for which the complex potential is

$$(2.12) \quad w = \xi + i\eta = \sinh^{-1} z.$$

For subcritical nozzle flows, it is appropriate to assume the asymptotic incompressible field for  $x$  or  $\xi$  large,

$$(2.13) \quad \psi = k\eta,$$

where  $k = \psi_w/\eta_w$ ,  $\psi_w$  being the mass flux. If the velocity potential is used as the dependent variable instead of  $\psi$ , the analogous condition along  $AD$  and  $BC$  is

$$(2.13') \quad \phi = k\xi.$$

ii) *The external flow of uniform stream over a body* (Fig. 2).

We have sketched the flow over a circular cylinder of unit radius as a typical body, and the incompressible potential solution in question is, for a free stream velocity parallel to the  $x$ -axis,

$$(2.14) \quad w = \xi + i\eta = z + \frac{1}{z}.$$

Because of symmetry, only the upper half of both the physical and working planes need to be drawn. Clearly,  $\frac{\partial \psi}{\partial \eta} = 0$  along  $ABCDE$ . On the outer contour  $EFGA$  the conditions again may be complicated because of the possibility of shocks in the domain. Consider for simplicity only subsonic uniform stream of  $q = U$ ,  $\rho = \rho_\infty$  at infinity. Then we may again assign

$$(2.15) \quad \psi = \frac{\rho_\infty}{\rho_0} \frac{U}{c_0} \eta \quad \text{or} \quad \phi = \frac{U}{c_0} \xi$$

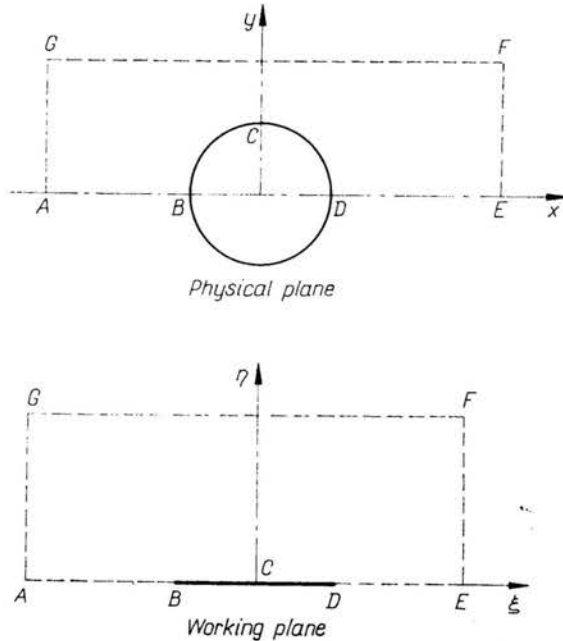


FIG. 2. Physical and working planes; circular cylinder.

along  $EFGA$ , by choosing the contour to lie sufficiently far from the body ( $BCD$ ). Better accuracy could be achieved by prescribing the appropriate asymptotic solution along  $EFGA$ . Its effects will be shown later.

**2.2. The streamline perturbation approximation**

The implication of the conditions (Eq. (2.13) or (2.15)) is none other than that the incompressible flow pattern should again prevail at large distances. In the working  $\xi, \eta$ -plane, not only the boundaries are rectified but the problem may be regarded as that of a channel between parallel walls, governed by Eq. (2.9) or (2.10), where the physical body enters only through effects of the incompressible velocity field in the density term. The streamlines are therefore expected to be approximately horizontal everywhere, and a thin-airfoil type of approximation immediately suggests itself. Both EMMONS [19] and MEKSYN [20] have already proceeded this way.

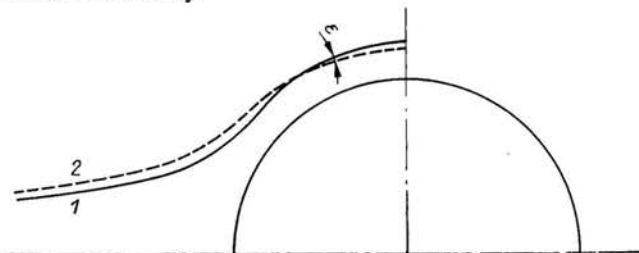


FIG. 3. Streamline perturbation due to compressibility.  
 1) — compressible streamline, 2) --- incompressible streamline.

Let  $\varepsilon$  be the angle between the streamlines with and without the compressibility effects, evaluated in the physical plane, as shown in the sketch of Fig. 3. Using Eq. (2.7), we readily find

$$(2.16) \quad \tan \varepsilon = -\frac{\psi_\xi}{\psi_\eta}$$

and shall assume  $|\varepsilon| \ll 1$ . Now Eq. (2.9) can be written as

$$(2.17) \quad A_1 \psi_{\xi\xi} + B_1 \psi_{\xi\eta} + C_1 \psi_{\eta\eta} + D_1 = 0,$$

where

$$(2.18) \quad \begin{aligned} A_1 &= \psi_\xi^2 + (1-M^2)\psi_\eta^2 \\ B_1 &= 2M^2\psi_\xi\psi_\eta, \\ C_1 &= (1-M^2)\psi_\xi^2 + \psi_\eta^2, \\ D_1 &= M^2(\psi_\xi^2 + \psi_\eta^2) \left( \psi_\xi \frac{Q_\xi}{Q} + \psi_\eta \frac{Q_\eta}{Q} \right). \end{aligned}$$

Substitution of Eq. (2.16) into Eq. (2.17) and deletion of terms of the order of  $O(\varepsilon^2)$  and smaller leads to

$$(2.19) \quad (1-M^2)\psi_{\xi\xi} + \psi_{\eta\eta} + M^2 \left( \frac{\psi_\xi Q_\xi + \psi_\eta Q_\eta}{Q} \right) = 0,$$

which agrees with EMMONS' approximate equation [19] to the order of  $O(\varepsilon)$ . Here  $M$  is the local Mach number, and the body shape enters in the incompressible speed ratio  $Q$ .

In a similar manner, Eq. (2.10) can be rewritten as

$$(2.20) \quad A_2 \phi_{\xi\xi} + B_2 \phi_{\xi\eta} + C_2 \phi_{\eta\eta} + D_2 = 0,$$

where

$$(2.21) \quad \begin{aligned} A_2 &= (1-M^2)\phi_\xi^2 + \phi_\eta^2, \\ B_2 &= -2M^2\phi_\xi\phi_\eta, \\ C_2 &= \phi_\xi^2 + (1-M^2)\phi_\eta^2, \\ D_2 &= -M^2(\phi_\xi^2 + \phi_\eta^2) \left( \frac{\phi_\xi Q_\xi + \phi_\eta Q_\eta}{Q} \right). \end{aligned}$$

It is easily verified that

$$(2.16') \quad \tan \varepsilon = \frac{\phi_\xi}{\phi_\eta}$$

and omitting terms of  $O(\varepsilon^2)$  in Eq. (2.20) leads to

$$(2.22) \quad (1-M^2)\phi_{\xi\xi} + \phi_{\eta\eta} - M^2 \left( \frac{\phi_\xi Q_\xi + \phi_\eta Q_\eta}{Q} \right) = 0$$

as the alternative to Eq. (2.19). MEKSYN's first approximation [20] results from omitting the term  $\phi_\eta Q_\eta$ , of  $O(\varepsilon)$ , in Eq. (2.22).

Further calculations need an explicit expression for the local Mach number  $M$ . In terms of  $\psi$ , we have from Bernoulli's equation,

$$(2.23) \quad M \left( 1 + \frac{\gamma-1}{2} M^2 \right)^{-\frac{\gamma+1}{2(\gamma-1)}} = \frac{\rho q}{\rho_0 c_0} = Q(\psi_\xi^2 + \psi_\eta^2)^{1/2}$$

hence, for  $|\varepsilon| \ll 1$ ,

$$(2.23') \quad M \left( 1 + \frac{\gamma-1}{2} M^2 \right)^{-\frac{\gamma+1}{2(\gamma-1)}} = Q\psi_\eta.$$

In terms of  $\phi$ , a simpler relation holds

$$(2.24) \quad M \left( 1 + \frac{\gamma-1}{2} M^2 \right)^{-\frac{1}{2}} = \frac{q}{c_0} = Q(\phi_\xi^2 + \phi_\eta^2)^{1/2},$$

hence, for  $|\varepsilon| \ll 1$ .

$$(2.24') \quad M \left( 1 + \frac{\gamma-1}{2} M^2 \right)^{-\frac{1}{2}} = Q\phi_\xi.$$

We shall refer to the pair of Eqs. (2.19) and (2.22) as the stream function formulation, or  $\psi$ -form for brevity, and the pair of Eqs. (2.21) and (2.23') as the velocity potential formulation, or  $\phi$ -form for brevity. Either pair can be used. The  $\psi$ -form takes Dirichlet boundary conditions on the solid body, but requires careful handling of Eq. (2.22) in the transonic region because of the choking phenomenon associated with the maximum of  $\rho q$  vs.  $M$ . Experience shows that it works well for numerical solution so long as in all iterations the local Mach number never exceeds unity. The  $\phi$ -form takes Neumann boundary conditions on the solid body. It turns out to be preferable in numerical calculations when locally supersonic pockets appear, as the monotonic nature of the variation of  $q$  vs.  $M$  in Eq. (2.23') can be iterated in a straightforward manner regardless of whether  $M \geq 1$ . In fact, the simplicity of Eq. (2.23) yields the explicit expression of  $M^2$ , which will be exploited later.

### 3. The finite element treatment

The finite element method is basically to discretize the solution of a field problem through local approximations and suitable integral constraints. The latter are preferably obtained by recasting the governing differential equation into a variational form. For the two-dimensional compressible potential flows in question, the variational principles due to Bateman are wellknown; see, e.g., the review by RASMUSSEN [21]. In the form of Eqs. (2.1) and (2.2), since  $\rho = \rho(q^2)$ , the operators are in fact „potential” and the following variational statements apply:

a) For Eq. (2.1)

$$(3.1) \quad \begin{aligned} \delta I_1(\psi) &= \delta \int_A \left( \int \frac{1}{\rho} dq^2 \right) dA - \oint_{\partial A} \frac{1}{\rho} \delta\psi \frac{\partial\psi}{\partial n} ds \\ &= 0; \end{aligned}$$



b) For Eq. (2.2)

$$(3.2) \quad \delta I_2(\phi) = \delta \int_A \left( \int \rho dq^2 \right) dA - \oint_{\partial A} \rho \delta \phi \frac{\partial \phi}{\partial n} ds = 0,$$

where  $A$  is the domain of interest,  $\partial A$  its boundary,  $ds$  the arc length along  $\partial A$ , and  $n$  the outward normal direction. These can be constructed following VAINBERG [22] and have already been pointed out by GELDER [23]. The variations are to be taken on  $\psi$  and  $\phi$ , respectively. Owing to the transcendental nature of the integrand in the area integrals, the implementation for computation is rather inconvenient. A straightforward iterative scheme would be to treat  $\rho$  as a given field quantity and subdue it in successive approximation, in the manner of TAYLOR and SHARMAN [24] fifty years ago. It is already better that the Poisson iteration mentioned in the "Introduction". An even more successful way of iteration has been reported by SHEN and HABASHI [16]. For working with Eq. (2.9) or (2.10) in  $\xi, \eta$ -coordinates, obviously Eqs. (3.1) and (2.21) are still valid with the proper interpretation.

A direct approach by the Galerkin procedure mathematically amounts to the construction of a weak solution. Briefly, consider Eqs. (2.19) and (2.21), both being of the type

$$(3.3) \quad (K_1 F_x)_x + (K_2 F_y)_y + K_3 = 0,$$

where  $K_1, K_2$ , and  $K_3$  are functions of  $F, F_x, F_y, x, y$ . We seek an approximate solution  $\hat{F}, \hat{K}_1, \hat{K}_2, \hat{K}_3$  as

$$(3.4) \quad \hat{F} = N_i(x, y) F_i, \quad \hat{K}_1 = N_i(x, y) K_{1i}, \quad \text{etc.},$$

in term of chosen known base functions  $N_i(x, y)$ , and unknown constant parameters  $F_i, K_{1i}, K_{2i}, K_{3i}$ . The summation convention is of course implied, and the number of the index  $i$  depends upon the desired accuracy. After proceeding in the usual way, a system of algebraic equations is obtained

$$(3.5) \quad \int_A (\hat{K}_1 N_{ix} \hat{F}_x + \hat{K}_2 N_{iy} \hat{F}_y - \hat{K}_3 N_i) dA - \oint_{\partial A} N_i (K_1 F_x l_x + K_2 F_y l_y) ds = 0,$$

where  $\hat{F}_x = N_{jx} F_j, \hat{F}_y = N_{jy} F_j, l_x$  and  $l_y$  are the direction cosines of the outward normal at  $ds$  along the contour  $\partial A$ . Eq. (3.5) may also be regarded as the result of the variational formulation in solving Eq. (3.3) iteratively, by evaluating  $K_1, K_2$  and  $K_3$  from the last iteration of  $F$ . Hence the boundary integral of Eq. (3.5) should be calculated from the imposed values of  $F, F_x$  and  $F_y$ .

The essential feature of the finite element method lies in subdividing the domain  $A$  into finite-sized elements and employing localized base functions  $N_i(x, y)$  that vanish except in the immediate neighbouring elements sharing a common "node". Eq. (3.5) is then applied to each element first, and the results are assembled. For general discussions on the choice of  $N_i$ , the assembling process and other details, see the books by ZIENKIEWICZ [25], GALLAGHER [26], and STRANG and FIX [27].

In the system resulting from Eq. (3.5), the forcing term determining the solution arises from the boundary integral around  $\partial A$ . It is therefore clear that the boundary value problem should be a well-posed one, and the governing differential equation should be

elliptic. In parts of the domain where the flow becomes supersonic, attention must be paid to reformulation of problem, for instance, carrying out the finite element discretization only in the "space-like" directions normal to the streamline. Such a semi-discrete finite element approach resembles closely the method of integral relations. However, the greater flexibility in the finite-element method allows one to patch together local solutions each of which may be constructed according to its own peculiarities. Singularities and asymptotic behaviours may be often described analytically; their judicious use will significantly increase the effectiveness of the numerical method.

### 3.1. The nozzle problem

We start with the Emmons nozzle (Fig. 1), which is formed by two hyperbolas according to Eq. (2.11) with  $\eta_w = 0.6$ , i.e.,

$$y^2 - x^2 \tan^2 0.6 = \sin^2 0.6.$$

The complex potential Eq. (2.12) provides both the mapping between the physical  $x, y$  and working  $\xi, \eta$ -planes, and the incompressible speed ratio explicitly:

$$(3.6) \quad Q = \left( \frac{2}{\cosh 2\xi + \cos 2\eta} \right)^{1/2}.$$

We shall proceed with the  $\psi$ -formulation, Eqs. (2.19) and (2.22).

Consistent with the streamline perturbation concept, we write for an assigned flux  $\psi_w$

$$(3.7) \quad \psi = k(\eta + \Psi),$$

where  $\Psi$  is the perturbation, and  $k = \psi_w/\eta_w$ .

Eq. (2.19) becomes an equation for  $\Psi$ ,

$$(3.8) \quad (1 - M^2)\Psi_{\xi\xi} + \Psi_{\eta\eta} + M^2 \left[ (1 + \Psi_\eta) \frac{Q_\eta}{Q} + \Psi_\xi \frac{Q_\xi}{Q} \right] = 0,$$

while Eq. (2.22') turns into

$$(3.9) \quad M \left( 1 + \frac{\gamma-1}{2} M^2 \right)^{-\frac{\gamma+1}{2(\gamma-1)}} = kQ(1 + \Psi_\eta).$$

For subcritical flows, because of the symmetry of the flow pattern only the solution in a quadrant of the  $\xi, \eta$ -plane needs to be computed. The boundary conditions, as discussed earlier, become

$$(3.10) \quad \begin{aligned} \text{i)} \quad & \Psi = 0 \quad \text{along} \quad \eta = 0, \quad \eta = \eta_w, \\ \text{ii)} \quad & \Psi_\xi = 0 \quad \text{along} \quad \xi = 0, \\ \text{iii)} \quad & \Psi = 0 \quad \text{along} \quad \xi = \xi_a, \end{aligned}$$

where at the station  $\xi = \xi_a$ , the incompressible field is assumed to hold. EMMONS [19] chose  $\eta_w = 0.6$ ,  $\xi_a = 1.35$  in his computations. These values are retained in our calculations so that the results may be compared.

It is now observed that a finite element program devised for Eqs. (3.8), (3.9) and (3.10) is in fact applicable for a much wider class of nozzles, not at all restricted to the particular hyperbolic shape studied by Emmons. The nozzle shape only needs to be such that the

corresponding incompressible flow may be assumed to have constant pressure across its entrance section and parallel streamlines at its exit, or, by reversing the flow direction, parallel streamlines at entrance and constant pressure at exit. The shape of the nozzle plays its role through the incompressible speed  $Q$  (or, equivalently, the incompressible pressure field), and the parameter  $\eta_w$ , and the problem is completely determined for specified  $\psi_w$ . However, because  $\psi_w$  for a given nozzle and the stagnation sound speed  $c_0$  is bounded from above, more conveniently Emmons prescribes instead the Mach number at the origin  $\xi = \eta = 0$ , and the appropriate  $\psi_w$  is evaluated as a consequence.

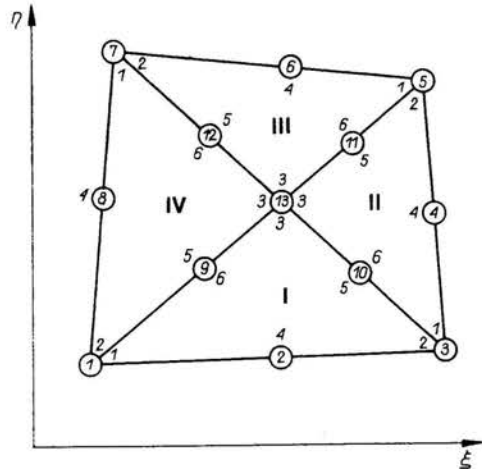


FIG. 4. Composition of 4 six-node triangles into a quadrilateral element.

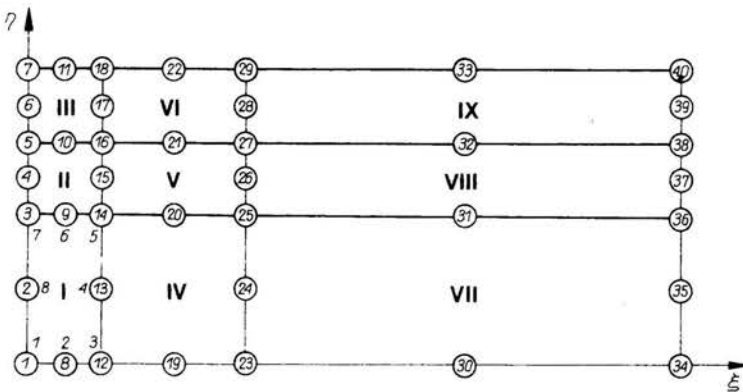


FIG. 5. Typical mesh layout for subsonic nozzle.

A finite element program has been developed for this case using quadrilateral elements, each consisting of four six-node triangles in which the unknown  $\psi$  is quadratically interpolated in term of the nodal values (Fig. 4). Elimination of the interior nodal unknowns (nodes 9 through 13) leaves a total of eight unknowns for each basic quadrilateral element. A typical  $3 \times 3$  layout in the  $\xi, \eta$ -plane with nine elements is shown as Fig. 5. The total number of nodal unknowns is 40, but 19 of them, along  $\eta = 0$ ,  $\eta = \eta_w$ , and  $\xi = \xi_a$  are

immediately set equal to zero according to (i) and (iii) of Eq. (3.10). The natural boundary condition  $\Psi_\xi = 0$  along  $\xi = 0$  is accounted for in the boundary integral of Eq. (3.5). The set of equations is then solved iteratively. Since the elements have only  $C^0$  continuity, after each iteration the derivatives at a nodal point evaluated from the adjacent elements are generally not in full agreement with one another. The usual practice is to assign simply the arithmetic average to be the representative value. With  $\Psi_\xi$  and  $\Psi_\eta$  thus determined, and the nodal Mach number following from Eq. (3.9), the functions  $K_1$ ,  $K_2$ , and  $K_3$  for the next iteration may then be evaluated. The convergence criterion is on the basis of the local values of either  $\Psi$  or  $M$ .

For the supercritical case, the flow enters subsonically but exist at supersonic speeds. We no longer have symmetry with respect to the  $\xi$ -axis, and must employ a marching procedure for the supersonic domain in the downstream direction. To circumvent the transonic throat region, a short-cut is to divide the flow into three "patches", with a small transonic patch describing the transition from subsonic to supersonic in the throat region. The upstream subsonic patch can be formulated as above with minor alterations; the downstream supersonic patch must be re-formulated into an initial value problem by applying the finite element discretization only in the  $\eta$ -direction. In the transonic patch, we take advantage of the known series solution due to OSWATITSCH [28] or its improved versions due to HALL [29], or KLIEGEL and LEVINE [30], to provide both the upstream boundary condition for the subsonic patch and the initial conditions for the supersonic patch. The results for the Emmons nozzle have been reported earlier [12]. Further details can be found in CHEN's thesis [16].

There remains the case when the flow is still subcritical, and symmetric with respect to the  $\xi$ -axis, but supersonic pockets form along the walls in the throat region. Strictly speaking we need to provide again a separate routine to handle the flow in the supersonic pocket as an initial value problem and patch it to the rest which is subsonic. EMMONS' treatment [19] of this difficulty is rather clever but ad hoc, and CHEN [16] has also succeeded in working out its counterpart in his finite element attack. The double-valued nature of  $M$  vs.  $q$ , Eq. (2.22), making the iteration particularly delicate in the neighbourhood of the sonic line, has to be handled with special care. In this respect, noting that the variation of  $M$  vs.  $q$ , Eq. (2.23), is always monotonic, it is definitely preferable in such circumstances to use the  $\phi$ -formulation as presented below.

### 3.2. Uniform flow over symmetrical bodies

Here we take the flow of a uniform stream of subsonic velocity over a circular cylinder as the pilot problem. Eq. (2.14) provides the mapping and the incompressible speed ratio is

$$(3.11) \quad Q = \left| 1 - \frac{1}{z^2} \right|.$$

With the  $\phi$ -formulation, the velocity potential is to be written as the sum of an asymptotic incompressible field plus a perturbation  $\Phi$ :

$$(3.12) \quad \phi = \frac{U}{c_0} (\xi + \Phi).$$

Restricted to shockless flows, again only one quadrant of the  $\xi, \eta$ -plane will be the domain of computation. Parallel to Eqs. (3.8) and (3.9), the governing equations are

$$(3.13) \quad (1 - M^2)\Phi_{\xi\xi} + \Phi_{\eta\eta} - M^2 \left[ (1 + \Phi_\xi) \frac{Q_\xi}{Q} + \Phi_\eta \frac{Q_\eta}{Q} \right] = 0$$

and

$$(3.14) \quad M \left( 1 + \frac{\gamma - 1}{2} M^2 \right)^{-\frac{1}{2}} = \frac{U}{c_0} Q(1 + \Phi_\xi).$$

In fact, Eq. (3.14) permits an explicit solution for  $M^2$  in terms of  $Q(1 + \Phi_\xi)$ , and by substituting the result in Eq. (3.13), we have, to  $O(\epsilon)$ ,

$$(3.15) \quad \left[ 1 - \frac{\gamma + 1}{2} \lambda^2 (1 + 2\Phi_\xi) \right] \Phi_{\xi\xi} + \left[ 1 - \frac{\gamma - 1}{2} \lambda^2 (1 + 2\Phi_\xi) \right] \Phi_{\eta\eta} - \lambda^2 Q [Q_\xi (1 + 3\Phi_\xi) + Q_\eta \Phi_\eta] = 0,$$

where

$$\lambda^2 = \frac{U^2}{c_0^2} = \frac{M_\infty^2}{1 + \frac{\gamma - 1}{2} M_\infty^2}.$$

An equation equivalent to Eq. (3.15) has been derived by CAUGHEY [3] in a finite difference method for airfoils.

The boundary conditions in Fig. 2 are

$$(3.16) \quad \begin{aligned} \text{i)} \quad & \Phi = 0 \quad \text{along} \quad EFGA, \\ \text{ii)} \quad & \Phi_\xi = 0 \quad \text{along} \quad \xi = 0, \\ \text{iii)} \quad & \Phi_\eta = 0 \quad \text{along} \quad \eta = 0. \end{aligned}$$

Condition (i) is of course a simplification since *EFGA* can never be at infinity in actual computation. It would be more accurate to prescribe the asymptotic behaviour of a doublet whose strength then enters at the nodes along *EFGA*, and is determined together with the rest of the nodal unknowns. As tested in Chen's thesis, with  $\xi$  and  $\eta$  equal 6 at *F*, the doublet term is found to have negligible influence on the results even at critical Mach number. (In lifting cases, the asymptotic logarithmic singularity due to circulation is of some significance; see SHEN [19], HABASHI [18]). Another alternative is to replace (i) by another Neumann condition,  $\Phi_\eta = 0$ , which will increase the number of unknowns slightly.

Thus, again, we see that Eq. (3.15) subjected to the homogeneous boundary conditions, Eq. (3.16), can be programmed once and for all, applicable to other body shapes that are symmetrical with respect to both the  $\xi$  and  $\eta$ -axes. For bodies symmetrical only with respect to the  $\xi$ -axis, an obvious and trivial modification of condition (ii) of Eq. (3.16) should be made, but the details need no elaboration. The body shape enters through  $Q$ , and the free stream Mach number through the parameter  $\lambda$ .

A finite element program has also been developed to handle such cases. The basic element chosen is the *BCIZ* nine-parameter cubic triangle, the parameters being the nodal values of  $\Phi$ ,  $\Phi_\xi$  and  $\Phi_\eta$  at the vertices. The velocity field follows without interpolation.

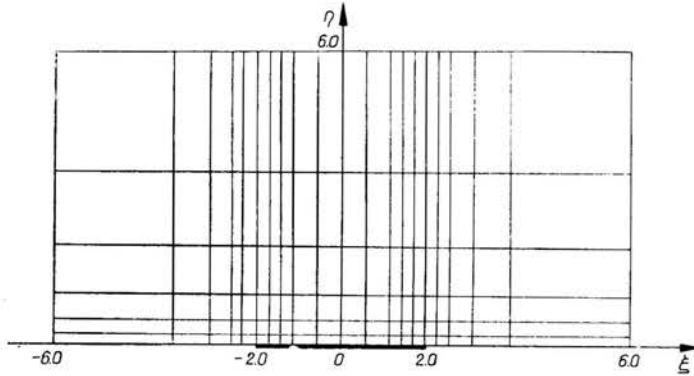


FIG. 6. Typical mesh layout for flow over a symmetrical body.

A typical layout is shown in Fig. 6, where the body is mapped to the line segment  $|\xi| \leq 2$ . The algebraic system resulting from Eq. (3.5) is solved iteratively, as in the  $\psi$ -formulation, through adjusting the corresponding coefficients  $K_1$ ,  $K_2$  and  $K_3$ .

#### 4. Calculated examples

##### 4.1. The Emmons' nozzle

With the  $\psi$ -formulation, six-node quadratic elements, and the  $3 \times 3$  mesh layout of Fig. 6, the computed results for the subcritical case of  $M = 0.692$  at the origin are compared with those due to EMMONS [19] in Fig. 7. The agreement is notable especially in view of the very small number of elements employed. Emmons' results are, of course, by no means exact. It is therefore also desirable to examine the discretization error of the finite

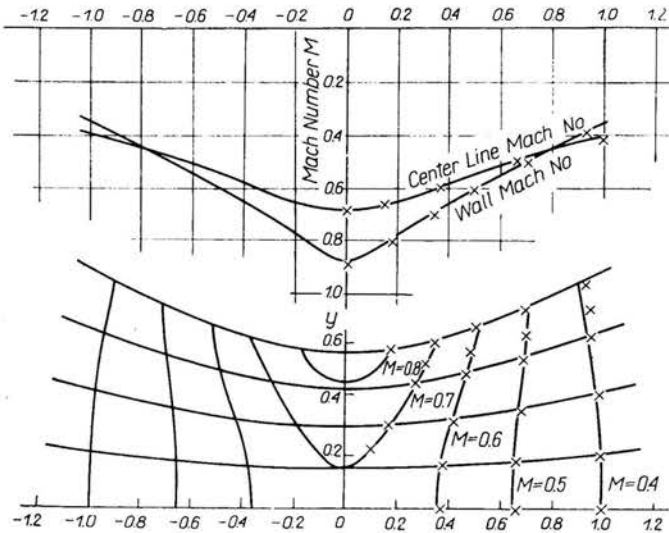


FIG. 7. Comparison of finite element solution with Emmons results;  $M = 0.692$  at origin.

elements analysis. A systematic mesh refinement starting with a  $2 \times 2$  layout, and successively halving it to  $4 \times 4$  and  $8 \times 8$  has been studied. The difference of the nodal stream function values between  $4 \times 4$  and  $8 \times 8$  appears to be within  $10^{-5} \times \psi_w$ .

Calculations for higher Mach numbers with the presence of a supersonic pocket at the walls and when the flow exits supersonically have also been made, but not with the standard program. Typical results have been presented before and are omitted here.

#### 4.2. Flow over a circular cylinder

The circular cylinder in a uniform stream has been the test problem for all kinds of methods treating compressible flows. In particular, the critical Mach number  $M_{cr}$  for the first appearance of the sonic point on the cylinder has been computed to a high degree of precision, see IMAI [31], SIMASAKI [32], and HOFFMAN [38], all based on the Rayleigh-Janzen series. In a six-term expansion Hoffman arrives at a value of  $0.3983 \pm 0.0002$ . Meanwhile, by using five strips in the method of integral relations, which is closely related to the semi-discrete finite element method alluded to above, MELNIK and IVES [7] arrive at  $M_{cr} = 0.39853 \pm 0.00002$ , in essential agreement with Hoffman's value. On the question whether a shockless supersonic pocket can exist over the cylinder at slightly higher Mach numbers, Hoffman estimates that the Rayleigh-Janzen series has a radius of convergence

$$M_{cr} \leq M < 1.055 M_{cr}.$$

Thus the lower bound may practically be at  $M_{cr}$ , and it may explain the convergence difficulty near  $M_{cr}$  in numerical schemes based upon the Poisson iteration where the source term represented the compressibility effects are determined through successive iteration. (This difficulty in fact has also been our experience with the finite element method [12, 16, 17]). However, in a velocity potential formulation and avoiding the approximation of the Laplace operator, HABASHI [17, 18] has been able to obtain shockless flows at  $M_\infty = 0.42$ .

In testing our program for the  $\psi$ -formulation, for low subsonic speeds up to  $M_\infty = 0.3$ , we use a  $7 \times 4$  grid in the quadrant, Fig. 8. There are 247 unknowns but reducible to 107 after static condensation. The circle lies between  $\xi = \pm 2$ , on which 9 nodes are placed, with smaller spacing near the stagnation point where the solution is expected to vary more rapidly. Starting from  $M_\infty = 0$  and marching progressively at Mach number steps of 0.1 to  $M_\infty = 0.3$ , we find that the program converges in 1 or 2 iterations to achieve a local Mach convergence of 0.001. For better accuracy of the result, especially at higher Mach numbers, the layout is then modified to a  $10 \times 7$  grid in the quadrant and the outer boundary extended to  $\xi = 6$  and  $\eta = 6$ . As in HABASHI [17], the first layer next to the cylinder is chosen to be very thin, i.e., at  $\eta = 0.05$ . The final number of unknowns is increased to 245. A typical result at  $M_\infty = 0.35$  is shown as Fig. 9, where IMAI's three-term approximation [31] is included for comparison. At  $M_\infty = 0.4$ , the asymptotic behaviour of a doublet of unknown strength  $A$  is added along the outer boundary chosen, and  $A$  is determined together with the nodal unknowns in the program. Our answer gives  $A = 1.089$ , while IMAI [34] has found it to be 1.10 from a three-term  $M_\infty^2$ -expansion.

The program for the  $\phi$ -formulation with cubic triangular elements is also tested on the circular cylinder. Here the layout is chosen to be  $20 \times 6$  in the half plane, again with body

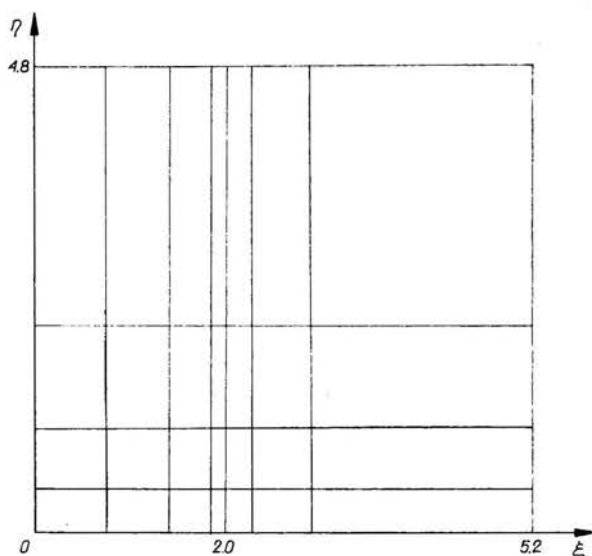


FIG. 8. Typical mesh layout for flow over cylinder,  $\psi$ -formulation.

between  $\xi = \pm 2$  and outer boundaries along  $\xi = \pm 6$ ,  $\eta = 6$ , Fig. 8. There are a total of 441 parameters, 39 of which are placed on the surface at 13 nodes. The major advantage over the  $\psi$ -formulation is the ease and accuracy to evaluate velocity and Mach number at the nodes, particularly significant at higher Mach numbers. In agreement with HABASHI [17, 18], no convergence difficulty is met up to  $M_\infty = 0.42$ , at which definitely one node becomes supersonic. We note that, according to Hoffman,  $M_\infty = 0.42$  is definitely at the upper bound of the Rayleigh-Janzen series. Further mesh refinement to ascertain the accuracy of the finite element solution, however, is yet to be done.

#### 4.3. Flow over ellipse and other symmetrical airfoils

Since body shape enters our program only through its incompressible speed ratio  $Q$ , the application to other bodies is readily made especially if the complex potential is analytically available. For high Mach number subsonic flows, the  $\phi$ -formulation should be the choice. We have computed several cases with the same program and mesh layout essentially as described above for the circular cylinder. For relatively thin bodies it is obviously important to use smaller mesh size near the stagnation points.

Following GREENSPAN and JAIN's finite-difference implementation of the variational principle [10], RASMUSSEN [11] has recently published results for high subsonic flows over an ellipse and a Kármán-Trefftz symmetrical airfoil with  $6^\circ$  trailing edge angle, both having a thickness ratio of 10%. In the case of the ellipse at  $M_\infty = 0.8$ , 357 unknowns are used and 1000 iterations are needed to reach 0.0001 convergence in the Mach number along the surface, and the computing time is reported to be 20 minutes on the IBM 360-65. For the same flow, our program with 447 unknowns turns out to require only 6 iterations



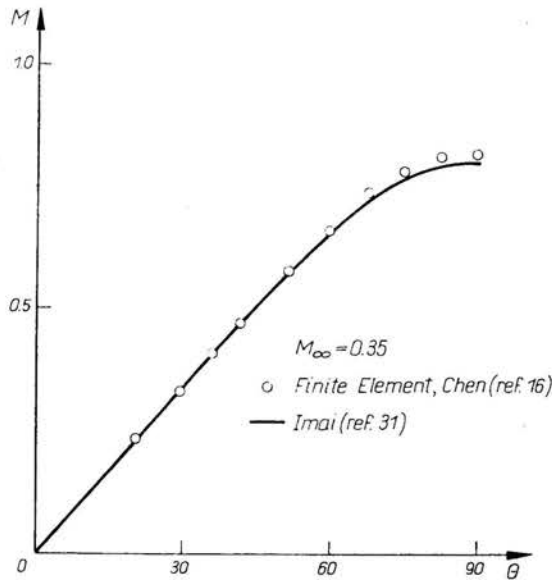


FIG. 9. Local Mach number at the surface of circular cylinder,

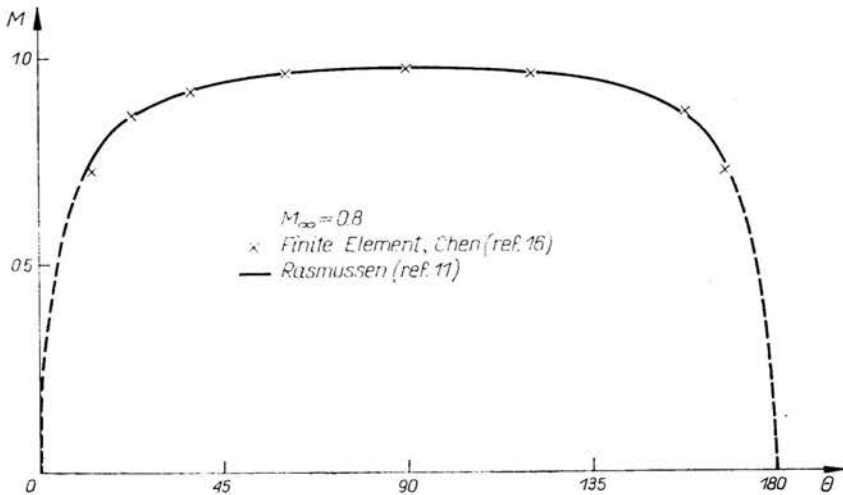


FIG. 10. Local Mach number at the surface of an ellipse, thickness ratio 10%.

for the same convergence criterion and 40 seconds on the IBM 370-168, equivalent to about 3 minutes on the IBM 360-65. Comparison of the computed results show excellent agreement in Fig. 10, where the abscissa is the angle on the mapping circle. The same agreement holds also at  $M_\infty = 0.82$ , when both show a supersonic pocket. A typical comparison for the flow over the Kármán-Trefftz airfoil is as in Fig. 11, where the solid line is due to RASMUSSEN [11], the free stream Mach number being 0.75. To fill in more points near the peak velocity, we put in extra nodes on the surface and the layout is changed to a  $24 \times 6$  grid work, with 525 unknowns.

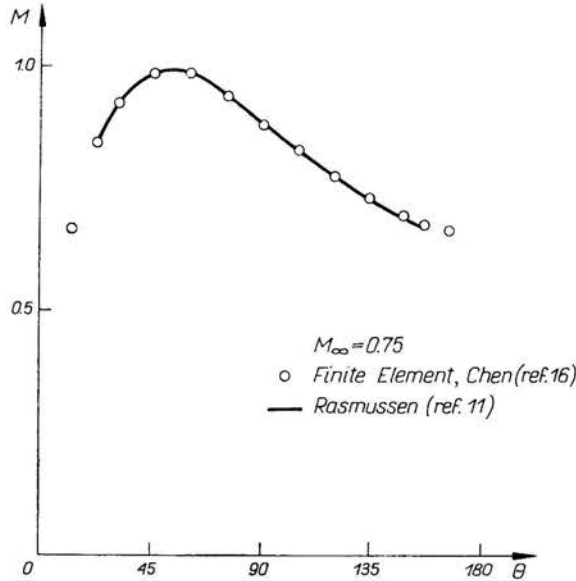


FIG. 11. Local Mach number at the surface of a Kármán-Trefftz airfoil with 6° trailing edge angle and 10% thickness ratio.

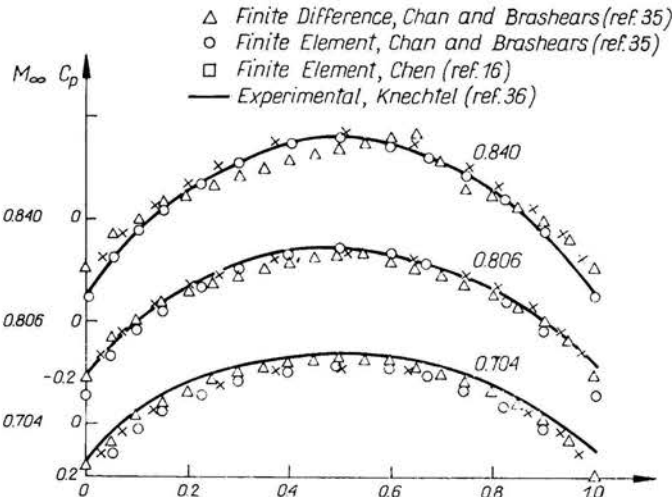


FIG. 12. Comparison of results for the 6% circular arc airfoil.

As a further example, the program is applied to a symmetrical circular arc airfoil of 6% thickness. At  $M_{\infty} = 0.774, 0.806$  and  $0.840$ , the results are compared in Fig. 12 with those from finite differences and the finite element calculation due to CHAN and BRASHEARS [35] and the experimental data of KNECHTEL [36]. Both the finite difference and the finite element calculations in Ref. [35] are based on the transonic perturbation equation for thin airfoils, while ours is free from such approximation. At the highest Mach number, it is probable that our results should be preferred.

## 5. Conclusions

The finite element programs described above, one for the stream function and the other for the velocity potential, are shown to be efficient and accurate in the calculation of high subsonic shockless flows including the occurrence of a supersonic pocket. Both are universal in the sense that the body shape enters in a simple manner through the incompressible speed ratio, or pressure field, which can be determined by other means which may be analytical, numerical, or experimental. For practical problems, the accuracy can be controlled through mesh refinement without revision of the program.

The success of the program is primarily due to the exploitation of the fact that the streamline pattern is rather weakly dependent on compressibility effects in the class of flows considered. Our perturbation equations can easily be carried to higher order, and no restriction on either the reference Mach number or the thickness of the body is necessary. The computation is done in the  $\xi, \eta$  plane so that full advantage may be taken of the simple form of the incompressible streamline pattern and essentially the same program covers both the nozzle flow and the flow over a body. In fact, for multiple bodies or wind tunnel interference problems, only a revision of the boundary conditions will suffice. Such is not the case for methods, like those of SELLS [3], MELNIK and IVES [7], or SATO [8], which map the computational domain into the interior of a circle.

Between the stream function and the velocity potential formulations, the latter should be preferred especially for high subsonic flows. The stream function program has a slight advantage for low subsonic flows where the Dirichlet type boundary conditions prevail. Because the local Mach number must successively be approximated through iterations, near the local sonic point, minor inaccuracy of the stream function will invariably cause difficulty. The velocity potential formulation is free from this trouble, and, in addition, the equation itself is simpler for numerical computation.

Although our programs predict the presence of supersonic pockets which are in agreement with the results of other computations for the examples considered, further study with refined mesh work in the supersonic pocket is of basic interest. It is not at all clear that as more elements become supersonic, the finite element formulation on the basis of a boundary value problem would not run into stability difficulty. Confidence in the accuracy of the details of the supersonic pocket must be established before the next crucial step of shockfitting can be attempted for transonic flows of still higher Mach number.

To pursue this objective, we should theoretically switch the program locally to a different routine that properly poses an initial value problem in the supersonic parts of the computation domain. Because of the flexibility of the finite element method it should be feasible to patch the local supersonic routine — by either line relaxation using finite differences or the method of integral relations, for example — to the main subsonic program. In the supersonic part, marching along the streamlines will be a key feature, and our choice of the rectangular grid in  $\xi, \eta$ -plane is clearly optimum for the procedure. In addition, the streamlines themselves are also characteristics, along which other information such as vorticity, entropy, etc. may be propagated in more complex situations. Their ease of identification becomes then even more significant, but in our formulation is already built-in for whatever body shape.

## Acknowledgment

This work has been supported by the U.S. Office of Naval Research under contract N00014-75-C-0375.

## References

1. E. M. MURMAN and J. D. COLE, *Calculation of plane steady transonic flows*, AIAA J., **9**, 114-121, 1971.
2. P. R. GARABEDIAN and D. G. KORN, *Numerical design of transonic airfoils*, Numerical Solution of Partial Differential Equations, II, Acad. Press, New York, 253-271, 1971.
3. C. C. L. SELLS, *Plane subcritical flow past a lifting airfoil*, Proc. Roy. Soc. London, **A308**, 377-401, 1968.
4. D. A. CAUGHEY, *An inviscid analysis of transonic, slatted airfoils*, AIAA Paper, 74-541, 1974.
5. T. C. TAI, *An application of the method of integral relations to transonic airfoil problems*, AIAA Paper, 71-98, 1971; *Transonic inviscid flows over lifting airfoils with embedded shock wave using method of integral relations*, AIAA Paper, 73-658, 1973.
6. M. HOLT and B. S. MASSON, *The calculation of high subsonic flow past bodies by the method of integral relations*, Proc. 2nd Int. Conf. Num. Methods in Fluid Dyn., Springer Verlag, Berlin, 207-214, 1971.
7. R. E. MELNIK and D. C. IVES, *Subcritical flow over two-dimensional airfoil by a multi-strip method of integral relations*, Proc. 2-nd Int. Conf. Num. Meth. in Fluid Dyn., Berkeley, Calif. 1970; Springer Verlag, Berlin, 243-251, 1971.
8. J. SATO, *Inverse method of designing two-dimensional transonic airfoils*, AIAA J., **11**, 1, 58-63, 1973.
9. C. T. WANG, *Variational method in the theory of compressible fluid*, J. Aero. Sc., **15**, 675-685, 1948.
10. D. GREENSPAN and P. JAIN, *Application of a method for approximating extremals of functionals to compressible subsonic flows*, J. Math. Anal. Appl., **18**, 85-111, 1967.
11. H. RASMUSSEN and N. HEYS, *Application of a variational method in plane compressible flow calculation*, J. Inst. Math. Appl., **13**, 47-61, 1974.
12. S. F. SHEN, *An aerodynamic looks at the finite element method*, Int. Symp. on Finite Element Methods in Flow Problems, Swansea, U. K., Jan. 1974; Chpt. 10, Finite Elements in Fluids, vol. 1, J. T. Oden, et al. (ed.), John Wiley, 1975.
13. J. H. ARGYRIS and G. MARECZEK, *Potential flow analysis by finite elements*, Ing. Archiv., **41**, 1-25, 1972.
14. D. H. NORRIE and G. de VRIES, *The finite element method*, Chapt. 15, Academic Press, 1973.
15. J. PERIAUX, *Two- and three-dimensional analysis of subsonic potential flows in ducts and around lifting bodies with finite element techniques*, Int. Symp. on Finite Element Methods in Flow Problems, J. T. Oden, et al. (ed) Univ. Alabama Press, 1974.
16. H. C. CHEN, *Applications of the finite element method to compressible flow problems*, Ph. D. Thesis (Aerospace Eng.), Cornell Univ., 1976.
17. S. F. SHEN and W. HABASHI, *Local linearization of the finite element method and its application to compressible flows*, First Int. Conf. on Computational Methods in Non-linear Mechanics, Austin, Texas, Sept. 1974; Int. J. Num. Methods in Eng., **10**, 565-577, 1976.
18. W. HABASHI, *A study of the finite element method for aerodynamic applications*, Ph. D. Thesis (Aerospace Eng.), Cornell Univ., 1975.
19. H. W. EMMONS, *The theoretical flow of a frictionless, adiabatic, perfect gas inside of a two-dimensional hyperbolic nozzle*, NACA TN 1003, 1946.
20. D. MEKSYN, *Integration of the equations of transonic flow in two-dimensions*, Proc. Roy. Soc., London, **A**, 220, 1953.
21. H. RASMUSSEN, *A review of the applications of variational methods in compressible flow calculations*, RAE Tech. Rept., 71234, 1971.

22. M. M. VAINBERG, *Variational methods for the study of non-linear operators*, Holden-Day, San Francisco 1964.
23. D. GELDER, *Solution of the compressible flow equations*, Int. J. Num. Methods in Eng., **3**, 35-43, 1971.
24. G. I. TAYLOR and C. F. SHARMAN, *A mechanical method for solving problems of flow in compressible fluids*, Proc. Roy. Soc., London, A, **121**, 1928.
25. O. C. ZIENKIEWICZ, *The finite element method in engineering science*, McGraw Hill, London, 1971.
26. R. H. GALLAGHER, *Finite element analysis. Fundamentals*, Prentice-Hall, N. J. 1974.
27. G. STRANG and G. J. FIX, *An analysis of the finite element method*, Prentice-Hall, N. J. 1973.
28. K. OSWATISCH, *Gas dynamics*, Acad. Press, N. Y. 1956.
29. I. M. HALL, *Transonic flow in two-dimensional and axially-symmetric nozzles*, Quart. J. Mech. Appl. Math., **15**, 4, 487-508, 1962.
30. J. R. KLIEGEL and J. N. LEVINE, *Transonic flow in small throat radius of curvature nozzles*, AIAA J., **7**, 1375-1378, 1969.
31. I. IMAI, *On the flow of compressible fluid past a circular cylinder*, Proc. Phys. and Math. Soc. Japan, Series 3, **20**, 636-645, 1938; *On the flow of compressible fluid past a circular cylinder, II*, Proc. Phys. and Math. Soc. Japan, Series 3, **23**, 180-193, 1941.
32. T. SIMASAKI, *On the flow of a compressible fluid past a circular cylinder, II*, Bull. Naniwa Univ., Series A, **4**, 27-35, 1956.
33. G. H. HOFFMAN, *Extension of perturbation series by computer. Symmetric subsonic potential flow past a circle*, J. de Mécanique, **13**, 433-447, 1974.
34. I. IMAI, *On the asymptotic behaviour of compressible fluid flow at a great distance from a cylinder in the absence of circulation*, J. Phys. Soc. Japan. **8**, 534-544, 1953.
35. S. T. K. CHAN and M. R. BRASHEARS, *Finite element analysis of transonic flow by the method of weighted residuals*, AIAA paper 75-79, 1975.
36. E. D. KNECHTEL, *Experimental investigation at transonic speed of pressure distributions over wedge and circular arc airfoil section and evaluation of perforated-wall interference*, NASA TN D-15, 1959.

CORNELL UNIVERSITY, ITHACA, NEW YORK 14853.

Received October 31, 1975.